Drainage of Packed Beds in Gravitational and Centrifugal-force Fields

EMILE NENNIGER, JR., and J. ANDERSON STORROW

University of Manchester, Manchester, England

The basic differential equations are developed for the prediction of saturation-time curves for the drainage of packed beds in either gravitational or centrifugal fields. The only mathematical solution existing at present, a series solution, is provided for these equations. A film drainage function is included to describe the movement of liquid along the surface of the particles when the main liquid level has passed through the pores of the bed. This method of analysis has been used successfully to predict the drainage of packed beds in a 9-in.-diameter hydroextractor. The important value of capillary suction head is best found from ancillary tests with Haines apparatus, but the value can be found with reasonable accuracy from the change in drainage rate as the liquid surface enters the upper surface of the packed bed. When these two rates are available, the permeability can also be found, and all the major variables are obtained from the drainage test on either the hydroextractor cake or the packed bed under gravity drainage.

Previous work (*35*) dealt with the problem of the movement of liquid through hydroextractor cakes in a centrifugal-force field (*16* to *21*, *23*, *24*) when the interstices of the packed bed were filled with liquid. For analysis of a complete hydroextraction cycle, it is necessary to obtain the equations governing the flow of liquid from a packed bed under drainage conditions when the voids are not filled with liquid. It should then be possible to integrate these two hydrodynamic processes over the appropriate portions of the cycle under the accelerating or decelerating fields while the cake is formed, washed, and "whizzed". The preliminary study of the spin-drying of cakes (*22*) showed that cake deformations and liquid distributions reduced the value of analyses based on samples cut from the hydroextractor cake. The two major problems were to measure the moisture content of a cake during spinning without liquid feed and to derive appropriate mathematical forms for analyses of experimental data. The solution to this problem has been provided (*31*) in the form of a series solution until the integrated form of the saturation-time function is available. The analysis has followed the necessary steps to apply functions for the bulk drainage of full pores and the film drainage across the walls of open pores toward the saturation limit at infinite time. This limit is set by the capillary suction head retaining a column of liquid that fills the pores at the base of the bed and the permanent liquid held by surface tension in the menisci at the interstitial contact points within the bed. The functions proposed have proved successful in both gravitational and centrifugal-force fields for a wide range of liquids and packed beds.

E. Nenniger is with Surveyer, Nenniger and Chênevert, Montreal, Canada, and J. Anderson Storrow with the Levington Research Station, Levington, Ipswich, England.

I. DRAINAGE OF PACKED BEDS IN A GRAVITATIONAL FIELD

LIQUID RETENTION IN PACKED BEDS

Liquid will be retained in a packed bed for any finite-force field, as (1) a saturated zone of capillary moisture stands above the datum of the outlet face of the bed, and (2) the drained portion of the bed will contain permanent residual liquid, i.e., liquid in menisci held at points of contact between bed particles.

Capillary Height in Packed Beds

The specification of capillary moisture depends on the statement of capillary height h_c of the vertical saturated column. The saturated zone due to capillary rise of liquid in packed beds, for instance in soil, and the time equations for upward infiltration from a lower source are known (*5*, *11*, *12*, *13*, *28*, *37*).

Haines (*14*, *15*), in applying surface-tension theory to spherical packing arrangements, predicted and found a difference in capillary height depending on whether the liquid was rising or falling within the bed. His experimental results for the latter in soils and those of Puri (*33*) for sands show an average value of $6\gamma/r$. Batel (*3*) suggested

$$h_c = C_1 \frac{2\gamma \cos \alpha}{\rho} \frac{1}{G} \left[\frac{d_m + d_h}{2} \right]^{1.2} \quad (1)$$

which includes particle-size distribution.

Dombrowski and Brownell (*8*) correlated capillary height h_c with a capillary drain number

$$Z = \left(\frac{K}{g}\right)^{\frac{1}{2}} \left[\frac{\rho G + \Delta P/L'}{\gamma/g \cdot \cos \alpha} \right]$$

finding a relation

$$h_c = 0.275/Z \quad (2)$$

Their data for gravity drainage from spherical particles and those of Uren and Difrawi (*36*) for capillary rise agree fairly well with Equation (2). The absence of the hysteresis mentioned by Haines may be a result of an overestimation of h_c due to the visual technique of Uren and Difrawi. The form of the capillary drain number has been confirmed by an analysis (*31*) based on Poiseuilles' equation for laminar motion in a capillary, Darcy's law, and the equation for capillary rise in a small tube. Recent experimental work (*31*) has shown good agreement with Equation (2) for beds of spherical particles and poor agreement for beds of kieselguhr and chalk. This leads to the conclusion that for spherical particles the Dombrowski

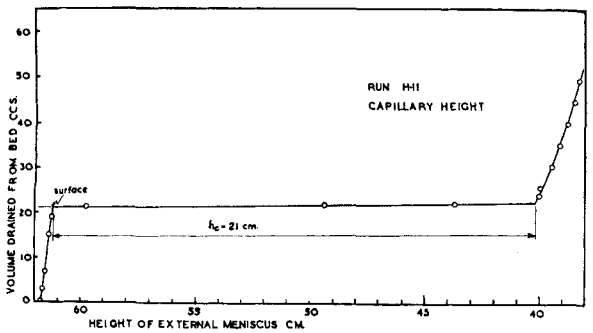

Fig. 1. Capillary height measured by Haine's technique.

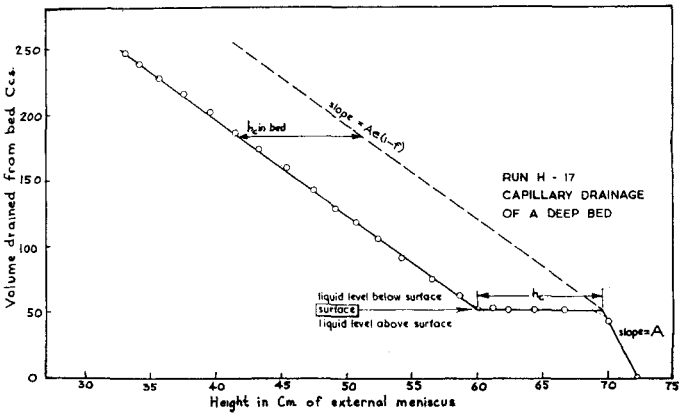

Fig. 2. Capillary drainage of a deep bed.

equation may be used, but for others h_c must be measured.

Experimental

The capillary height h_c for various packed materials was measured with a Haines apparatus for liquids of various surface tensions. Figure 1 shows a typical test for 0.036-cm.-diameter spheres with distilled water, the suction necessary to drag the liquid down into the bed being equivalent to a water-column h_c of 21 cm. A major premise in the development of the drainage equation is that h_c is a constant retarding force throughout the bed. Figure 2, which is the result of a Haines run on a deep bed, shows experimental proof of this. Moving from right to left as the liquid surface falls to the bed level, the slope corresponds to the area A of the open tube. As the liquid attempts to enter the bed, a suction of h_c is required. Thereafter the liquid falls through the bed following a line of constant slope which corresponds to the free pore volume of the drained bed. Since sufficient time elapsed between readings (30 min.) to eliminate dynamic effects, the residual moisture in the drained pores was constant, and, therefore, the capillary height h_c was constant and equal to the entry value of the bed.

Permanent Residual Liquid

The retention of liquid at contact points in a packed bed has not been analyzed in detail. Ferguson (*10*) has solved the case for a sphere in contact with a horizontal liquid surface, and Bashforth and Adams (*1*) have provided a lengthy step-by-step solution to the case of drops resting on a horizontal plane. Batel (*2*) has considered the problem for two spheres in horizontal contact, but a misapplication of the Laplace surface-tension equation seems to have been made, and his development is applicable only to two long cylinders in contact.

Brownell and Katz (*4*) correlated residual liquid (capillary liquid included) with the capillary number

$$Z_0 = \frac{K\Delta P}{g\gamma L'}$$

giving the equation

$$S_r = \frac{Z_0^{-0.264}}{86.3} \qquad (3)$$

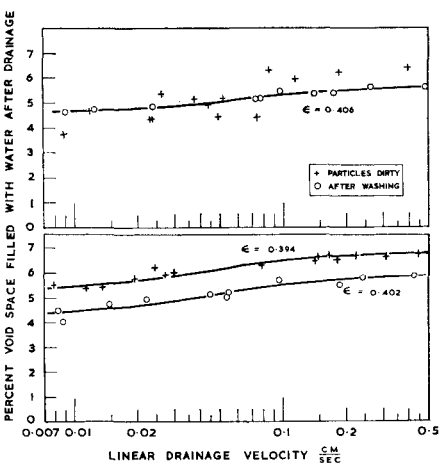

Fig. 3. Effect of drainage velocity on residual moisture in a packed bed of glass spheres with average particle diameter of 0.26 cm.

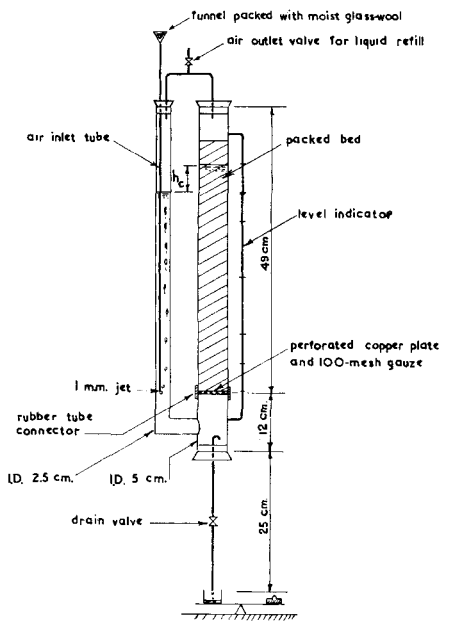

Fig. 4. Constant drainage-velocity apparatus for deep beds.

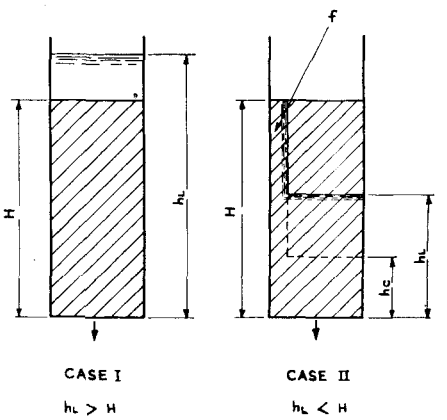

Fig. 5. Simple model of drainage mechanism in a packed bed.

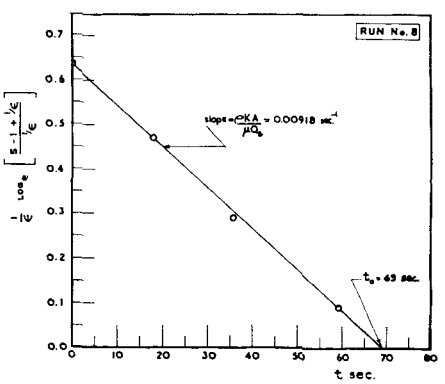

Fig. 6. Evaluation of permeability function in Equation (9).

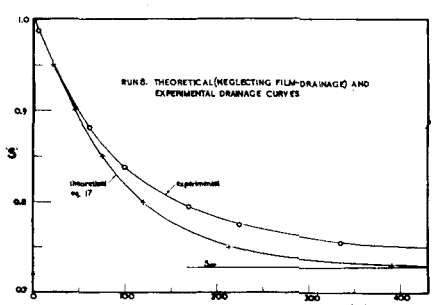

Fig. 7. Comparison of experimental drainage curves with theoretical equation (17), film drainage neglected.

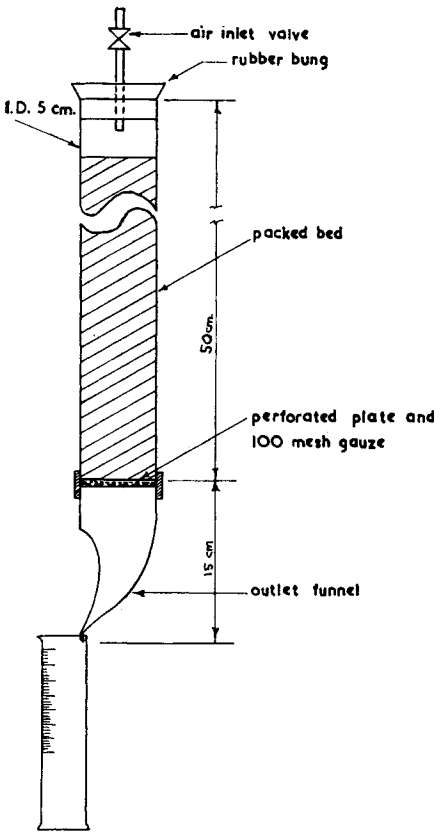

Fig. 8. Gravity drainage apparatus for deep beds.

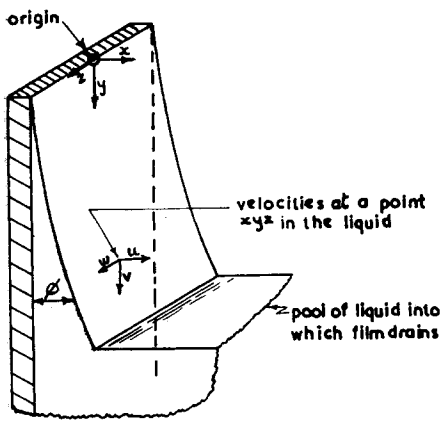

Fig. 9. Theoretical model of film drainage.

Dombrowski and Brownell (*8*) suggested that the permanent residual liquid never rises much above 7½% when Z_0 lies between 10^{-6} and unity, excluding moisture absorbed in the particles themselves. This is dubious. Keen (*27*), in an analysis of wedge moisture between spheres, showed that fusion would occur with an f value of 18.2 and 24.3% for the most open and closest packing arrangements respectively. This condition presumably must arise somewhere in the above-mentioned range of Z_0.

Batel (*3*) has suggested an equation which on analysis (*31*) reduces to

$$f = k_5 Z_0^{-0.25} \qquad (4)$$

This is similar to the Brownell equation (*3*) except that k_5 is an unknown function of porosity of the bed and sphericity of the particles. Experimental data are too few to allow a final choice between Equations (3) and (4).

Experimental

Observation of the meniscus formed between two 1-cm. glass spheres in vertical contact was made through a Vernier microscope. The volumes of the menisci formed from various liquids were measured by means of a corrected form of the equation stated by DallaValle (*7*). During these experiments a slight effect of formation velocity on meniscus size was noted. This effect was further tested by measuring the liquid retention in packed beds after lowering the liquid surface through a position of the bed at a fixed rate.

Constant Drainage-Velocity Apparatus

The apparatus in Figure 4 provided a constant pressure drop across the drain valve while the drainage of the bed proceeded, thus maintaining a constant drainage velocity for a given valve setting. An external level indicator showed an arbitrary level for the liquid in the bed, the indicated level differing from the actual level because of the difference of capillary effect in the bed and in the indicator tube. This difference was constant for a specific packed bed.

The permanent residual moisture in 39-cm.-deep beds of 0.26-cm.-diameter glass spheres and 33-cm.-deep beds of 1.00-cm.-diameter glass spheres was measured by weighing the drainage from the beds. The times allowed for drainage were generally considerably longer than the period from Equation (23) for the reduction of unstable-film drainage liquid to 0.1% of the void volume.

Results

Figure 3 shows data for 0.26-cm. glass spheres after drainage had ceased, the results being expressed as f, the fraction of the voids remaining filled. The influence of small amounts of dirt in the bed is shown by the lack of reproducibility. There was also a marked influence of changes in bed porosity.

DEVELOPMENT OF DRAINAGE EQUATIONS WITH FILM DRAINAGE NEGLECTED

The first steps in the formation of equations for the flow of liquid within the packed bed were based on the laminar movement of liquid as the liquid surface at h_L fell toward the upper surface of the bed at height H above the outlet datum (Figure 5), followed by a flow through the bed as h_L moved from H down to the final capillary height h_c. The pressure is taken as atmospheric at the surface h_L and at the datum of the outlet face.

Case when $h_L > H$

For laminar motion through the bed

$$-\frac{dQ}{dt} = \frac{h_L}{H}\frac{\rho K A}{\mu} \qquad (5)$$

$$Q = Q_s + (h_L - H)A \qquad (6)$$

whence

$$-\frac{dQ}{dt} = \left[\frac{Q - Q_s + HA}{HA}\right]\frac{\rho K A}{\mu} \qquad (7)$$

Expressing the moisture content as the fraction, $S = Q/Q_s$, of the voidage yields

$$-\frac{dS}{dt} = \left[\frac{S - 1 + 1/\epsilon}{1/\epsilon}\right]\frac{\rho K A}{\mu Q_s} \qquad (8)$$

Integrating this equation between the limits $S = S$ at $t = t$ and $S = 1$ when $t = t_0$ as the liquid level reaches the surface of the bed gives

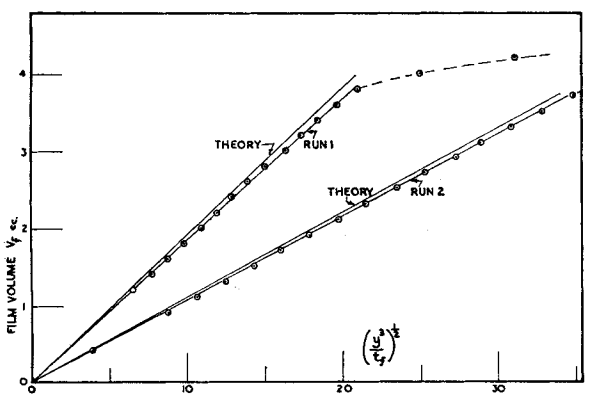

Fig. 10. Film drainage in a 50-ml. burette as a test of Equation (23).

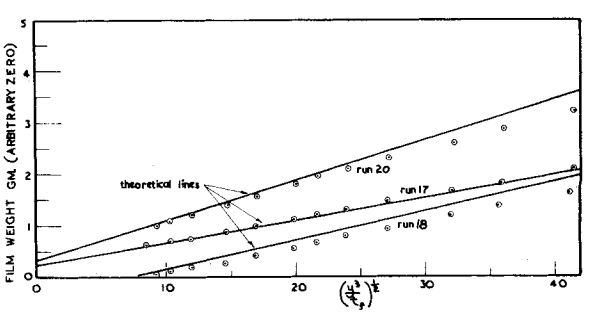

Fig. 11. Drainage of oil films from vertical strings of beads compared with Equation (23), with $L = \pi d$.

$$\log_e \left[\frac{S - 1 + 1/\epsilon}{1/\epsilon}\right] = \frac{\epsilon \rho K A}{\mu Q_s}(t_0 - t) \qquad (9)$$

This equation can be used to analyze data to give K, and to define t_0 as shown in Figure 6.

Case when $H > h_L > h_c$

Neglecting any film drainage on a surface exposed by the falling-liquid surface, one may base an equation for this case on the following assumptions:

1. K is constant for all positions in the submerged bed
2. The capillary force retards the drainage from the bed with a force equal to suction height h_c, which is constant for all positions of the liquid surface within the bed.
3. The permanent residual liquid in the bed above the liquid surface is of constant f throughout the drained portion of the bed
4. The equivalent of flow equation (5) applies to the moving fluid in the submerged part of the bed
5. Deceleration forces may be neglected in the slow changes of mean velocity in the liquid.

$$-\frac{dQ}{dt} = \left(\frac{h_L - h_c}{h_L}\right)\frac{\rho K A}{\mu} \qquad (10)$$

$$Q = h_L A \epsilon + (H - h_L) A \epsilon f \qquad (11)$$

whence

$$-\frac{dQ}{dt} = \left[\frac{Q - HA\epsilon f - h_c A \epsilon (1-f)}{Q - HA\epsilon f}\right]\frac{\rho K A}{\mu} \qquad (12)$$

The integration of Equation (12) may be simplified by substituting the terms Q_s, Q_c and Q_∞ for the values of saturated volume, capillary-height volume, and final liquid volume respectively, where

$$Q_\infty = (H - h_c) A \epsilon f + h_c A \epsilon \qquad (13)$$

$$Q_c = h_c A \epsilon \qquad (14)$$

$$Q_s = HA\epsilon. \qquad (15)$$

Integrating the expression between $Q = Q_s$ at $t = t_0$ and $Q = Q$ at $t = t$, when $t > t_0$ gives

$$Q_s - Q + Q_c(1 - f) \log_e \left[\frac{Q_s - Q_\infty}{Q - Q_\infty}\right] = \frac{\rho K A}{\mu}(t - t_0) \qquad (16)$$

or in terms of saturated fraction, S

$$1 - S + S_c(1 - f) \log_e \left[\frac{1 - S_\infty}{S - S_\infty}\right] = \frac{\rho K A}{\mu Q_s}(t - t_0) \qquad (17)$$

It may be observed that the gradient of the S, t curve is independent of f when the bed is saturated, that is, when $Q = Q_s$ and $S = 1$:

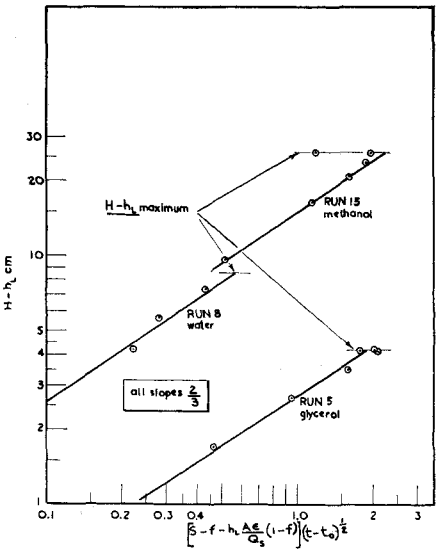

Fig. 12. Film-drainage test on gravity-drainage runs with packed beds.

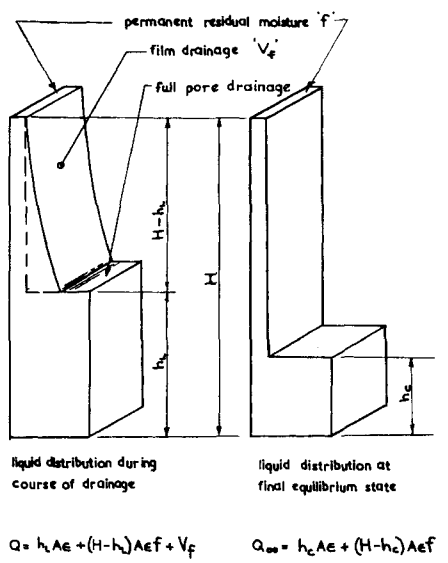

Fig. 13. Models of liquid distribution in packed bed.

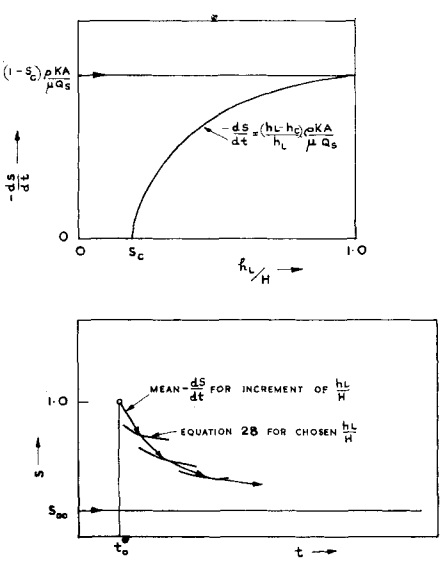

Fig. 14. Method of graphical integration combining Equations (24) and (28).

$$-\frac{dQ}{dt} = \left[\frac{Q_s - Q_c}{Q_s}\right]\frac{\rho K A}{\mu} \qquad (18)$$

$$-\frac{dS}{dt} = (1 - S_c)\frac{\rho K A}{\mu Q_s} \qquad (19)$$

Equations (18) and (19) may be used to evaluate the capillary suction height h_c from Q_c or S_c provided that it is a reasonable fraction of the bed and that the permeability K is known accurately.

Batel (3) also derived an equation similar to Equation (17) but discussed it only qualitatively. The foregoing equations were tested for drainage of water, water-glycerol solutions, ethyl alcohol, and methyl alcohol on various beds of glass spheres. The drainage rates when $h_L > H$ were analyzed by Equation (9), providing a measure of K and the time when the liquid reached the bed surface. The S, t function was drawn on a large scale and (dS/dt) found for $S = 1$ to evaluate h_c. The difference in dS/dt just above and below the limit $h_L = H$ is marked. Above the limit

$$-\frac{dS}{dt} = \frac{\rho K A}{\mu Q_s}, \text{ when } h_L \to H \qquad (20)$$

whereas a lower value from Equation (19) is obtained when h_L is just below H. The values for h_c compared within 5% with values found from Haines apparatus for beds of spheres 0.036 cm. in diameter. Although this drainage technique can be used for h_c determination, the Haines technique is more accurate. The permanent residual moisture f was found from Equation (13) and the S, t curve calculated from Equation (17). The deviation of the experimental data from this theoretical equation is exemplified in Figure 7. Calculation showed that it was justifiable to neglect the kinetic head change on the liquid entering the bed and that the flow regime was laminar. All tests showed the same discrepancies; the theoretical Equation (17) predicted a more rapid approach to the final state than was found.

There are two possible explanations for this: either variation in suction height h_c as the surface falls through the bed, or film drainage of liquid from the packing above the surface. Although the constancy of h_c with position in pure liquids has been proved experimentally, a very marked effect did occur in the presence of surface-active agents. It is well known that liquids containing surface-active agents display variations in surface tension under dynamic conditions, owing to the significant time required for molecular orientation at freshly formed surfaces. The variation in dynamic surface tension gives the effect of a false h_c, falling toward the value of h_c measured in the slow movements of a Haines test. In slow drainage tests at constant rate with surface-active agents, the variation in h_c is not observed, the value for h_c as

in Figure 2 remaining constant at all positions in the bed, with $h_c \propto 1/\gamma$ and having the same value as found at the bed surface.

This effect cannot be detected with pure liquids, and the explanation of the delay in bed drainage appeared to be the presence of film drainage over the exposed surfaces of the packing above the liquid surface. The effect was sufficiently significant to require a modification of Equation (17). The dynamic surface-tension problem need not be considered further in the present study, which is confined to liquids which did not contain active surface agents. The predominant deviating influence from the model (Figure 5) giving Equation (17) was undoubtedly the presence of film drainage of liquid across the surfaces of the packing after the liquid level had passed through the bed.

Gravity Drainage Apparatus

The apparatus used for run 5 consisted of a small cylindrical cell of diameter 4.9 cm. and depth 10 cm., with 100-mesh copper gauze used as a bed support. The cell was hung from a glass cantilever, the deflection of which was followed by a capacitance recorder.

Runs 7 to 16 were carried out on deeper beds in the simple apparatus shown in Figure 8, the outlet funnel being designed to minimize liquid holdup and to give smooth flow. The drainage-volume rate was obtained by timing the level in the volumetric measuring receiver through manual operation of an electrical marker on a fast ticker tape as the level passed calibration marks. Beds were made by dumping packing into the tube filled with liquid. Care was required to avoid disturbances of the tube contents which could favor a definite size distribution vertically in the bed, with consequent variations in h_c. To start a run it was necessary only to turn the air valve to the full open position.

DEVELOPMENT OF FILM DRAINAGE THEORY

A modifying function is required to include the effect of film drainage in the S, t function. Jeffreys (*26*) published an approximate solution to the Stokes-Navier equation for film drainage from a vertical plane. His expression for the liquid profile as a function of time may be integrated to give the volume of liquid in the film varying with time.

The Stokes-Navier equation for an incompressible fluid falling down a vertical plane reduces to

$$-\rho g = \mu \frac{\partial^2 v}{\partial x^2} \qquad (21)$$

if it is assumed that for the coordinates in Figure 9,

(1) no forces act horizontally along the z direction; $\partial v/\partial z = 0$, $\partial^2 v/\partial z^2 = 0$, $w = 0$

(2) velocity in the x direction is small; $u \rightarrow 0$

(3) change in vertical velocity with height is small; $\partial v/\partial y \rightarrow 0$, and its rate of change is small; $\partial^2 v/\partial y^2 \rightarrow 0$

(4) vertical acceleration is negligible except near the start of drainage; $\partial v/\partial t \rightarrow 0$, $t_f \neq 0$

Equation (21) has been applied as an approximation to similar problems by Nusselt (*32*) and by Kocatas and Cornell (*29*). The expression obtained by Jeffreys for the film thickness at a given level y is

$$\phi = \sqrt{\frac{\mu y}{\rho g t_f}} \qquad (22)$$

This expression may be integrated to give the volume of the film V_f at time t_f when y is the height of the top of the film above the pool into which it drains. For breadth of film L,

$$\partial V_f = L\phi \, \partial y$$

$$V_f = \frac{2}{3} L \sqrt{\frac{\mu y^3}{\rho g t_f}} \qquad (23)$$

Jeffreys did not test his equation (22). Morey (*30*) applied the form to evaluate the correction for wet gas meters and found better agreement with an exponent of 0.63 rather than 0.5. It seemed necessary to test these equations by the drainage of vertical surfaces.

The application to vertical walls is clear from the bases of derivation, with the expectation that the equations will fail in the initial stages of a film formation when accelerations are significant. The application to packed beds must rest on the assumption that the only major difference occurs in the interpretation of the significant breadth of film L.

Film-drainage Experiments

Initial experiments were conducted on the drainage of the wall of a 50-ml. glass burette, which effectively provided a plain wall. The liquid level in the burette was dropped rapidly from the top to the bottom graduation. The upward movement of the meniscus was then timed by observation through a traveling microscope. The results are shown in Figure 10 with V_f as a function of t_f and y. Run 1 for $\mu/\rho = 689$ centistokes shows the deviation from the equation expected by Jeffreys during the rapid acceleration period over a short time. The remaining points over periods up to hours fitted the gradient $\frac{2}{3} L(\mu/\rho g)^{1/2}$ within 3 to 4%. The experimental measurements gave the liquid drained from the film, and the first run was allowed to proceed for 60 hr. to obtain residual V_f for $t_f = \infty$, enabling the calculation of the true variable V_f value for each t_f. The data in run 2 showed similar agreement for a liquid of kinematic viscosity of 228 centistokes. Apart from a very short time at the start, the film drainage from a vertical plane agrees well with Equation (23).

Experiments were also made with vertical strings of spherical beads. The string was dipped in oils of various viscosities and immediately hung on a steel-rod cantilever. The deflection of this beam was followed by a high-frequency capacitance recorder, the record being available from calibration as a weight-time function for the drainage from the vertical string of beads. The mean effective breadth L of the vertical plane is difficult to specify, and equally so is the detailed function of the flow throughout the film draining over the beads. As an approximation, a value of L was taken as the mean surface area of the dry beads divided by the height of the string, that is, effectively πd. Results were analyzed by plotting an arbitrary weight against $(y^3/t_f)^{1/2}$, giving graphs such as in Figure 11. The rectilinearity of the plots confirmed the power of 0.5 and the near agreement with Equation (23). Data for eighteen runs with kinematic viscosities ranging from 150 to 700 centistokes showed an average agreement within 10% with Equation (23) and no significant variation with kinematic viscosity of the liquid. The variation of 10% around Equation (23) is not important in view of the fact that the drainage function is to be a modification to the main flow equation for liquid moving through the immersed voids. Hewitt (*25*), in allied work on the drainage of tower packing, has found agreement to 3 to 7% using a similar basis for L. He has used the initial condition as liquid flowing over the packing in a steady state. In the bead experiments the initial state is disturbed by the effective increase in gravitational field when the bead string is withdrawn rapidly from the oil. Again the form of Equation (23) appears satisfactory after a short initial period in the drainage.

Preliminary Test of Film Drainage in Packed Beds

In packed beds the presence of film drainage does not influence the driving-force Equation (10), which may be written

$$-\frac{dS}{dt} = \frac{\rho K A}{\mu Q_s} \frac{(h_L - h_c)}{h_L} \qquad (24)$$

but the material-balance Equation (11) must now accommodate the draining film:

$$Q = h_L A\epsilon + (H - h_L) f A\epsilon + \frac{Q_s B (H - h_L)^{\frac{3}{2}}}{\sqrt{t_f}} \qquad (25)$$

where B is a constant for a specific liquid and packing. From Equation (25), dividing through by Q_s and rearranging gives

$$\left[S - f - \frac{h_L A\epsilon(1 - f)}{Q_s}\right]\sqrt{t_f} = B(H - h_L)^{\frac{3}{2}} \qquad (26)$$

From the drainage run for a packed bed giving an S, t curve, the first derivative at any time allows the calculation of h_L and $(H - h_L)$ from Equation (24). These values, inserted in the groups of Equation (26), give the plot in Figure 12. Data for various liquids in a packing of glass spheres appear to conform to Equation (26), but it will be noticed that the data become more erratic at high $(H - h_L)$ values, where $h_L \rightarrow h_c$ and $t_f = (t - t_0) \rightarrow \infty$, owing to the difficulty of measuring dS/dt accurately. The agreement is such that the use of the Jeffreys form of film-drainage equation is justified in packed-bed analysis, despite its inadequacy for a short time after film drainage starts.

Complete Drainage Equation

The model now becomes as in Figure 13, with the conditions for Equation (11) modified by the presence of V_f expressed as

$$V_f = \frac{2}{3} L \sqrt{\frac{\mu(H - h_L)^3}{\rho g(t - t_0)}} \qquad (27)$$

$$L = s_0 A$$

and thus S at any time becomes

$$S = \frac{h_L}{H}(1 - f) + f + \frac{2}{3}\frac{s_0}{\epsilon}\sqrt{\frac{H\mu}{\rho g}}\sqrt{\frac{(1 - h_L/H)^3}{(t - t_0)}} \qquad (28)$$

This equation and Equation (24) form the bases for the complete drainage equation for the packed bed in a gravitational field.

Graphical Integration

The integration of these equations has not yet been solved, but two approaches have proved successful. A graphical integration was performed to test the equations for a specific run by plotting the quadratic equations for S against $(t - t_0)$ for various h_L/H. For decrements in S, starting from $S = 1$ at $t = t_0$, a mean slope from Equation (24) was used to draw a straight line to a (S, t) curve for the smaller value h_L/H; a progressive use of this approximation shown in Figure 14 provided the S, t curve. Figure 15 shows the comparison between the calculated and experimental data.

This method was tedious, but it served to show that the equations gave a satisfactory solution to the whole drainage problem.

Series Solution

In default of a successful integration, a series-solution method has been adopted. It is of advantage to simplify the equations for this purpose by letting

$$a = \frac{h_c}{H}\frac{\rho K A}{\mu Q_s} \qquad (29)$$

$$b = \frac{\rho K A}{\mu Q_s} \qquad (30)$$

$$p = (1 - f) \qquad (31)$$

$$k_1 = \frac{2}{3}\frac{s_0}{\epsilon}\sqrt{\frac{H\mu}{\rho g}} \qquad (32)$$

$$X = \left[1 - \frac{h_L}{H}\right] \qquad (33)$$

Substitution in Equations (24) and (28) leads to

$$\frac{dS}{dt} = \frac{a}{1 - X} - b \qquad (34)$$

$$S = 1 - pX + k_1\left[\frac{X^3}{t - t_0}\right]^{\frac{1}{2}} \qquad (35)$$

where all the terms are positive. It should be noted that Equations (34) and (35) are the two basic differential equations. For any specific case, a, b, p, and k_1 are constants.

To eliminate S and find X, the equations can be solved for the case when $k_1 = 0$, and then a correction introduced for the film drainage. The values of S can then be estimated.

Case when $k_1 = 0$

Combining Equations (34) and (35) and integrating with $X = 0$ when $t = t_0$ and with $X = X$ when $t = t$ gives

$$(t - t_0) = \frac{p}{b}\left[X - \frac{a}{b}\log_e\left(1 - \frac{bX}{b - a}\right)\right] = \psi_0(X) \qquad (36)$$

$\psi_0(X)$ can be expressed as a series

$$\psi_0(X) = a_1X + a_2X^2 + a_3X^3 + \cdots \qquad (37)$$

The values of a_1, a_2, etc., can be obtained by expanding the logarithm in Equation (36) and equating coefficients

$$a_1 = p/(b - a) \qquad (38)$$

$$a_2 = pa/2(b - a)^2 \qquad (38a)$$

$$a_n = \frac{apb^{n-2}}{n(b - a)^n} \quad (n \neq 1) \qquad (38b)$$

The solution to Equations (24) and (28) is now based on $\psi_0(X)$ and expressed as a series.

Case with $k_1 \neq 0$

Equation (36) may be adjusted to the case when $k_1 \neq 0$ by the addition of another series in X. Then, by manipulating the equations and equating the coefficients, a general solution of the film drainage equations is obtained.

If

$$(t - t_0) = \chi_0(X) + \chi_1(X) \qquad (39)$$

and

$$\psi_1 = b_1X + b_2X^2 + b_3X^3 + \cdots \qquad (40)$$

combining Equation (34) with the differential dS/dX from Equation (35) gives

$$\left[\frac{a - b + bX}{1 - X}\right][\psi_0{}'(X) + \psi_1{}'(X)] = -p + k_1\frac{d}{dX}\left[\frac{X^3}{\psi_0 + \psi_1}\right]^{\frac{1}{2}} \qquad (41)$$

and substituting the value of p, from the first derivative of Equation (36), in Equation (41) yields

$$\left[\frac{a - b + bX}{1 - X}\right][\psi_1{}'(X)] = k_1\frac{d}{dX}\left[\frac{X^3}{\psi_0 + \psi_1}\right]^{\frac{1}{2}} \qquad (42)$$

It is an advantage to introduce a new series to reduce the right-hand side of Equation (42) to a form easier to handle.

If

$$\frac{X^3}{\psi_0 + \psi_1} = [c_1X + c_2X^2 + c_3X^3 + \cdots]^2 \qquad (43)$$

coefficients c_1, c_2, c_3 . . . must be evaluated in terms of a_1, a_2, a_3 . . . and b_1, b_2, b_3 . . . . Inserting Equations (37) and (40) in Equation (43) and equating coefficients of powers of X gives

$$c_1 = \sqrt{\frac{1}{a_1 + b_1}} \qquad (44)$$

and since $[X^3/(t - t_0)]^{1/2} > 0$, the positive root will be used.

$$c_2 = -\frac{a_2 + b_2}{2(a_1 + b_1)^{\frac{3}{2}}} \qquad (44a)$$

$$c_3 = \frac{3}{8}\frac{(a_2 + b_2)^2}{(a_1 + b_1)^{5/2}} - \frac{a_3 + b_3}{2(a_1 + b_1)^{\frac{3}{2}}} \qquad (44b)$$

From Equation (42) it is possible to write

$$(a - b + bX)(b_1 + 2b_2X + 3b_3X^3 + \cdots) = k_1(1 - X)[c_1 + 2c_2X + 3c_3X^2 + \cdots] \qquad (45)$$

Equating coefficients again gives the terms of the ψ_1 series as functions of the original constants in the basic equations.

Constant b_1

$$(a - b)b_1 = k_1c_1 \qquad (46)$$

and from Equations (38) and (44)

$$(b - a)^2b_1{}^3 + (b - a)pb_1{}^2 - k_1{}^2 = 0 \qquad (47)$$

where

$$(b - a) > 0$$

TABLE 1. SUMMARY OF PACKED-BED AND LIQUID PROPERTIES FOR GRAVITY DRAINAGE RUNS ON BEDS OF GLASS SPHERES

Run	d_m, cm.	H, cm.	A, sq. cm.	ϵ	Liquid	ρ, g./cc.	μ, poise	γ, dyne./cm.	h_c, cm.	f
5	0.26	6.2	18.9	0.415	Glycerol	1.25	4.72	66	2.08*	0.048
8	0.036	29.6	19.7	0.405	Water	1.00	0.010	73	21.1*	0.052
9	0.036	34.5	19.7	0.400	Water	1.00	0.010	73	20.5*	0.116
15	0.036	34.0	19.7	0.396	Methanol	0.796	0.00606	22.8	8.00†	0.146
16	0.036	33.6	18.8	0.408	Ethanol	0.793	0.0123	22	7.65†	0.127

*Measured in drainage apparatus, from Equation (19), by use of measured $-dS/dt$ at h_L just below H.
†Measured in similar bed in separate Haines capillary suction-height apparatus.

Constant b_2

$$b_2\left[2(a-b)+\frac{k_1}{(a_1+b_1)^{\frac{1}{3}}}\right] \quad (48)$$

$$=-bb_1-\frac{k_1a_2}{(a_1+b_1)^{\frac{1}{3}}}-\frac{k_1}{(a_1+b_1)^{\frac{1}{3}}}$$

Constant b_3

$$b_3\left[3(a-b)+\frac{3}{2}\frac{k_1}{(a_1+b_1)^{\frac{1}{3}}}\right]$$

$$=-2bb_2+\frac{9}{8}\frac{k_1(a_2+b_2)^2}{(a_1+b_1)^{5/2}}$$

$$-\frac{3}{2}\frac{k_1a_3}{(a_1+b_1)^{\frac{1}{3}}}+\frac{k_1(a_2+b_2)}{(a_1+b_1)^{\frac{1}{3}}} \quad (49)$$

More terms may be evaluated but in most cases only b_1 and b_2 are necessary to obtain an equation of accuracy comparable to the constants a, b, p, etc.

A slight problem arises in the calculation of the first term of the ψ_1 series, b_1. It requires the solution of a cubic equation (47), only one of the three roots being correct. The correct root is easy to select, and the limits of this root can be established.

The correct root b_1

The general pattern of Equation (46) is

$$\theta(b_1)=(b-a)^2b_1^3+(b-a)pb_1^2-k_1^2 \quad (50)$$

$$(b-a)>0$$

now

$$\theta(\infty)=\infty$$

$$\theta(-\infty)=-\infty$$

$$\theta(0)=-k_1^2$$

$$\theta[-p/(b-a)]=-k_1^2$$

The first derivative

$$\frac{d\theta}{db_1}=3(b-a)^2b_1^2+2(b-a)pb_1 \quad (51)$$

Now $d\theta/db_1=0$, when $b_1=0$

$$\frac{d\theta}{db_1}=0, \quad \text{when} \quad b_1=-\frac{2}{3}\frac{p}{b-a}$$

The second derivative

$$\frac{d^2\theta}{db_1^2}=6(b-a)^2b_1+2(b-a)p \quad (52)$$

and

$$\frac{d^2\theta}{db_1^2}=0 \quad \text{when} \quad b_1=\frac{1}{3}\frac{p}{b-a}$$

Thus there is a pattern with

(1) a point of inflection at $b_1=\frac{1}{3}p/(b-a)$
(2) a maximum at $b_1=-\frac{2}{3}p/(b-a)$
(3) a minimum at $b_1=0$

and the maximum value of θ is

$$\theta\left[-\frac{2}{3}\frac{p}{b-a}\right]=\frac{4}{27}\left(\frac{p^3}{b-a}\right)-k_1^2 \quad (53)$$

From Equation (46), b_1 must be negative since $(b-a)>0$ and $c_1>0$. It is therefore necessary to choose between the two negative roots for b_1 where $\theta(b_1)=0$. This can be done by considering Equation (47) for small values of k_1.

As $k_1\to 0$, then $\theta(b_1)\to(b-a)^2b_1^3+(b-a)pb_1^2\to 0$ which has roots $b_1=0$ and $b_1=p/(b-a)$. But as $k_1\to 0$, $\psi_1\to 0$, and, from Equation (39), then $b_1\to 0$, $b_2\to 0\ldots$. Thus the correct root for b_1 lies between $-\frac{2}{3}p/(b-a)$ and zero in all cases.

An interesting variation arises when there is no real root for b_1 between these limits. This means that $k_1^2>4/27\,(p^3)/(b-a)$. Analysis of this situation, including the Kozeny equation

$$s_0^2=k_4\frac{\epsilon^3}{5}\frac{g}{K} \quad (54)$$

shows that in this case

$$\frac{(1-f)^3}{(1-S_c)}>\frac{3}{5}$$

which is not a clear conclusion. It is tacitly assumed that this occurs when k_1^2 is large compared with the other variables, that is, when the film drainage is the dominant problem and the permeability is large, the level h_L approaching h_c in a very short time. In this event X will quickly assume its final value $(1-h_c/H)$ or $(1-S_c)$, and Equation (35) become

$$S=1-p(1-S_c)+k_1\left[\frac{(1-S_c)^3}{t-t_0}\right]^{\frac{1}{3}} \quad (55)$$

or

$$S=S_\infty+k_1\left[\frac{(1-S_c)^3}{t-t_0}\right]^{\frac{1}{3}} \quad (56)$$

Thus, when $k_1^2>4/27\,(p^3)/(b-a)$, Equation (56) may be used alone to describe the S, t function, with the caution that it does not hold when $(t-t_0)$ approaches zero.

Summary of Mathematical Solution

The mathematical solution gives the two simultaneous equations

$$(t-t_0)=\frac{p}{b}\left[X-\frac{a}{b}\log_e\left(1-\frac{bX}{b-a}\right)\right]+b_1X+b_2X^2+b_3X^3 \quad (57)$$

$$S=1-pX+k_1\left[\frac{X^3}{t-t_0}\right]^{\frac{1}{3}} \quad (35)$$

If $k_1=0$, then $b_1, b_2\ldots=0$, and the combination of these equations gives Equation (17). This solution for zero film drainage from the wetted packing is only a limit, all actual cases having $k_1>0$ and significant film drainage. Knowing the constants enumerated above makes it possible to find the relationship between t and X from Equation (57) and the S, t function by substitution in Equation (35).

EXPERIMENTAL RESULTS

Drainage in a Gravitational Field

The data for run 16 were calculated in this way and the results are plotted on Fig. 15. They show very good agreement with the experimental results. Another typical experimental result is shown in Figure 16, confirming the success of the proposed Equations (35, 57). The S, t curves with film drainage neglected are shown by plotting Equation (17), an indication of the significance of the film-drainage correction.

Experimental data for various liquids (Table 1) showed excellent agreement with the analysis proposed and appear to confirm the validity of both the series functions and the drainage model postulated. Until a suitable integrated solution is available for S, the series solution seems adequate. This method of solution may appear complicated, but the following example shows the method of procedure.

Example of drainage calculation

The conditions of the chosen problem correspond to those of run 5 except that the residual saturation $100f$ is taken as 7% instead of the experimental value of 5% to demonstrate that a small change in f will remove the discrepancy between the calculated and experimental values on

Figure 16 and give an exact fit. This adjustment is within the limit of experimental error in this case, as the permanent residual moisture $f = 0.05$ was measured on the electronic weighing balance after standing for several hours.

PROBLEM

Calculate the saturation of a bed with time when it is allowed to drain from fully saturated to the final equilibrium state. The capillary drain height h_c of this bed with the liquid used is 2.08 cm., the bed permeability K is 0.0647 cc./sec.^{2}, and the permanent residual moisture f is equivalent to 7%.

DATA

Bed

Type	glass ballotini
area, A	18.9 sq. cm.
Depth, H	6.2 cm.
Average particle size, d	2.6 mm.
Sphericity	1.0
Total void volume, Q_s	48.6 cc.
Voidage, ϵ	0.415
Liquid	glycerine and water
Density, ρ	1.25 g./cc.
Viscosity, μ	472 centipoise
Surface tension, γ	66 dynes/cm.

X	ψ_0	b_1X
0.0	0	0
0.1	21.6	−6.95
0.2	44.5	−13.9
0.3	69.7	−20.8
0.4	98.6	−27.8
0.5	135	−34.7
0.6	193	−41.7
0.64	244	−44.5
0.66	331	−45.8
0.663	395	−46

CALCULATION

(a) Calculation of Constants a, b, p, k_1, X_∞, a_1, a_2

From Equation (29), $a = 0.00224$ sec.$^{-1}$
From Equation (30), $b = 0.00668$ sec.$^{-1}$
From Equation (31), $p = 0.93$
From Equations (32) and (54), with k_4 taken as unity, $k^1 = 3.65$ sec.$^{1/2}$
From Equation (33), with $h_L = h_c$, $X_\infty = 0.664$
From Equation (38), $a_1 = 210$ sec.
From Equation (38a), $a_2 = 53$ sec.

X	$t - t_0 = \psi_0 + \psi_1$	pX
0.0	0	0
0.1	14.6	0.093
0.2	30.4	0.186
0.3	48.6	0.279
0.4	69.8	0.372
0.5	98.8	0.465
0.6	149	0.559
0.64	197	0.596
0.66	283	0.614
0.663	346	0.617

(b) Test for the Significance of Permeability

Equation (53) will be used to see whether there is a real value of b_1. If b_1 is imaginary, the simplified Equation (56) will be used for S. If b_1 is real, as in this case, the series solution will be used. Quantity b_1 is real since $4/27(p^3)/(b - a) - k_1^2 = 13.5$; i.e., > 0.

(c) Calculation of b_1, the First Term of the Series

The cubic equation (47) is solved for the root b_1, within the limits of zero and $-\frac{2}{3}(p)/(b - a) = -140$. The solution is $b_1 = -69.5$ sec.

(d) Calculation of b_2, the Second Term of the Series

From Equation (48) and the preceding value of b_1, the value of b_2 becomes −6.0 sec.

(e) Calculation of the X, t Curve

A number of X values are chosen between $X = 0$ and $X = X_\infty$, and for each of these t is calculated from Equation (57), which is more easily handled as

$$t - t_0 = \frac{p}{b}\left[X + S_c \log_e\left(\frac{X_\infty}{X_\infty - X}\right)\right] + b_1X + b_2X^2 + \cdots \qquad (57a)$$

With $t_0 = 0$, at the time the liquid leaves the surface, the following values result:

b_2X^2	ψ_1	$t = \psi_0 + \psi_1$
0	0	0
−0.06	−7.0	14.6
−0.24	−14.1	30.4
−0.36	−21.1	48.6
−0.96	−28.8	69.8
−1.5	−36.2	98.8
−2.2	−43.9	149
−2.5	−47	197
−2.6	−48	283
−2.6	−49	346

$$\psi_0 = \frac{p}{b}\left[X + S_c \log_e \frac{X_\infty}{X_\infty - X}\right]$$

These values show that it is sufficient to take the first two terms of the series, as the second term correction, $b_2 X^2$, amounts to only about 1% of the total time.

(f) Calculation of the S, t Curve

The saturation for any value of time and X calculated above may be obtained from Equation (35) by inserting the simultaneous values of X and $t - t_0$.

$1 - pX$	$k_1[X^3/t]^{1/2}$	S
1.00	0	1.00
0.907	0.030	0.937
0.814	0.059	0.873
0.721	0.086	0.807
0.628	0.111	0.739
0.535	0.129	0.664
0.441	0.139	0.580
0.404	0.133	0.537
0.386	0.116	0.502
0.383	0.106	0.489

The curve of saturation with time is shown in Figure 17. It is interesting to note that the largest value of X chosen for the calculation is very nearly that of the final value, and if it is required to extend the curve further in time, Equation (56) may be used alone. The agreement between experimental data and the calculated S, t function is shown to be satisfactory in Figure 17. The influence of the change of f from 5 to 7% is seen by comparison with Figure 16.

II. HYDROEXTRACTION: DRAINAGE OF PACKED BEDS IN CENTRIFUGAL FIELD

DRAINAGE IN A CENTRIFUGAL FIELD

A detailed analysis of the problem of drainage from a centrifuge cake would involve allowance for the variation with radial position of both centrifugal force and cross sectional area normal to the force. As the cake thickness is usually a small fraction of the basket radius, the use of constant mean values of the quantities will be sufficiently accurate:

$$A_m = \pi(r_c + r_0)Y \qquad (58)$$

$$G = \frac{2\pi^2 n^2 (r_c + r_0)}{g} \qquad (59)$$

The depth of cake perpendicular to the direction of flow and the location of liquid level may be expressed in terms of radii (Figure 18). Thus Equation (24) becomes

$$-\frac{dS}{dt} = \left[\frac{(r_0 - r_L) - h_c}{(r_0 - r_L)}\right]\frac{G\rho KA}{\mu Q_s} \qquad (60)$$

and Equation (28) becomes

$$S = \left(\frac{r_0 - r_L}{r_0 - r_c}\right)(1 - f) + f + \frac{2}{3}\frac{s_0}{\epsilon}\left[\frac{\mu(r_0 - r_c)}{\rho g G}\right]^{\frac{1}{2}} \left[\frac{\left[1 - \left(\frac{r_0 - r_L}{r_0 - r_c}\right)\right]^3}{t - t_0}\right]^{\frac{1}{2}} \qquad (61)$$

Equations (60) and (61) are of the same form as Equations (24) and (28), and the same series solution will apply.

$$a_c = \frac{h_c}{r_0 - r_c}\frac{G\rho KA}{\mu Q_s} \qquad (62)$$

$$b_c = \frac{G\rho KA}{\mu Q_s} \qquad (63)$$

$$p = (1 - f) \qquad (31)$$

$$k_c = \frac{2}{3}\frac{s_0}{\epsilon}\sqrt{\frac{(r_0 - r_c)\mu}{G\rho g}} \qquad (64)$$

$$X_c = 1 - \left(\frac{r_0 - r_L}{r_0 - r_c}\right) \qquad (65)$$

with these groups Equations (61) and (62) become

$$\frac{dS}{dt} = \frac{a_c}{1 - X_c} - b_c \qquad (66)$$

$$S = 1 - pX_c + k_c\left[\frac{X^3}{t - t_0}\right]^{\frac{1}{2}} \qquad (67)$$

and the series solution is

$$(t-t_0)=\frac{p}{b_c}\left[X_c-\frac{a}{b}\log_e\frac{X_\infty}{X_\infty-X_c}\right]+b_1X_c+b_2X_c^2+b_3X_c^3+\cdots \quad (68)$$

where b_1, b_2 . . . are defined as before.

EXPERIMENTAL RESULTS

Experiments were carried out on a 9-in.-diameter vertical-wall perforated-basket centrifuge with beds of chalk and of kieselguhr formed on duck-weave cloth (Table 2). Each cake was formed slowly from a dilute slurry maintained at constant concentration by recirculation to a feed tank to keep the particle-size distribution constant through the cake. The cake thickness was made uniform by disturbance of the adjacent liquid, and the permeability was measured by a probe technique as described previously (*16*). The method involves the measurement of the time Δt required for the liquid surface at $r_L < r_c$ to move from r_{L_1} to r_{L_2}, whence

$$\log_e\left[\frac{r_0^2-r_{L_1}^2}{r_0^2-r_{L_2}^2}\right]=\frac{4\pi^2n^2\rho K\Delta t}{\mu g\log_e r_0/r_c} \quad (69)$$

To measure the drainage, the cakes were allowed to drain to equilibrium at a constant centrifuge speed, the moisture content being found by stopping the centrifuge at intervals and weighing the whole basket and contents to determine the liquid loss. The permanent residual moisture was found in each run by the gravimetric analysis of a sample from the inner surface of the cake. This enabled the calculation of a capillary-drain height by a material balance on the final equilibrium state. The capillary suction height for the chalk material was very high, and consequently the cakes scarcely drained at all.

In Figure 19 the data for three tests on chalk show reasonable agreement with the series solution despite the crude method of obtaining the experimental S, t data. The specific surface per unit volume of bed was obtained for these cakes from the Kozeny Equation (54) without any correction factor, that is, $k_4 = 1$, ϵ ranging from 0.548 to 0.665. The drainage on curve 1C (Figure 19) is so small that h_c may have been greater

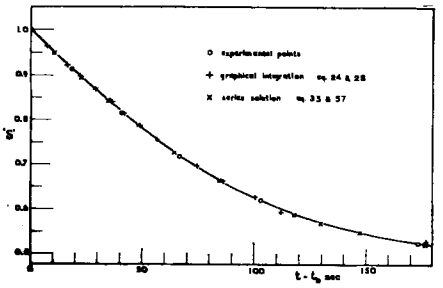

Fig. 15. Graphical integration and series solution for run 16.

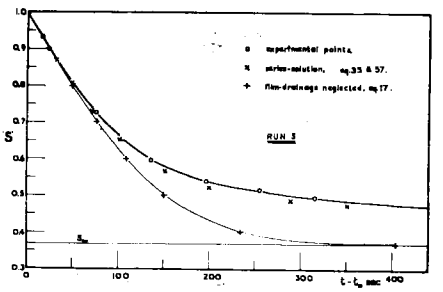

Fig. 16. Gravity drainage of glycerol from a packed bed.

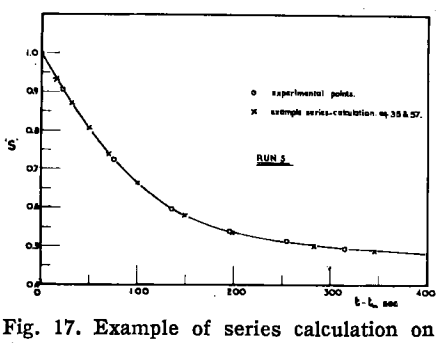

Fig. 17. Example of series calculation on data from run 5 with f equivalent to 7% for comparison with the data from f = 5% in Fig. 16.

than the cake thickness ($r_0 - r_c$). The small moisture loss of 1½% could have been due to the slight contraction of the cake as the liquid level penetrated the surface, although the probe survey did not show contraction within 1%.

The kieselguhr cakes had lower h_c values than the chalk and drained to lower S_∞ values, improving the accuracy of the tests. In each case the data showed that with the high permeability the film drainage was dominant. Thus the S, t curves were adequately expressed by

$$S = S_\infty + k_c\left[\frac{(1-S_c)^3}{t-t_0}\right]^{\frac{1}{2}} \quad (70)$$

A problem arose in the calculation of specific surface of these cakes owing to their high porosities of 0.825 to 0.840. Rose (*34*) suggests a correction factor of 9 or 10 on k_4 in Equation (54) when determining S_0 by the gas permeability method for porosities of this range. The calculated values in Figure 20 show good agreement with the experimental results when using a correction factor of 1.3 to the specific surface determined from liquid permeability.

CAPACITANCE APPARATUS

Capacitance Cell

The cell shown in Figure 21 consisted essentially of a 4-cm. length of 2.48-cm.-internal-diameter Perspex tube with a 100-mesh copper gauze fixed at the outer end to act as an earthed plate and as a support for the 0.036-cm.-diameter ballotini. A further copper gauze was fitted firmly over the bed with a Perspex slip ring to act as the live plate of the condenser. This gauze was in contact with the Fielden-Drimeter capacitance recorder through the mercury-pool contact in the Perspex centerpiece fixed to the axis of the hydroextractor bowl. The earthed contact through the aluminum basket was made by a brass screw to the gauze, and a rubbing ring was fitted to the top of the bowl. Care was taken in the construction to ensure that atmospheric pressure obtained at the outer gauze face of the cell, that is, at radius r_0 in Figure 21.

The constancy of calibration of the cell is shown in Figure 22*a*, which indicates the weight changes involved in a cell of dry weight 48.4 g. The corresponding saturation calibration curve is shown in Figure 22*b*.

Capacitance Method with Hydroextractor

This research ends the series of studies undertaken on hydroextraction problems. Thus it may be of interest to describe briefly the partial success of the attempt

Table 2. Summary of Cake Data for 9-in.-diameter Hydroextractor Drainage Runs

Outer radius of cake, r_0 = 11.3 cm.

Height of cake, Y = 11.8 cm.

Run	Material	r_c, cm.	Q_s, cc.	ϵ	$K \times 10^7$, cc./sec.²	N, rev./min.	G	f
1C	Chalk	9.58	736	0.548	0.421	1,820	—	—
2C	Chalk	8.81	1,226	0.665	1.12	1,820	372	0.53
3C	Chalk	8.87	1,119	0.620	0.995	2,380	637	0.445
4C	Kieselguhr	8.94	1,481	0.840	12.6	1,400	224	0.465
5C	Kieselguhr	9.46	1,173	0.825	13.0	1,440	240	0.57
6C	Kieselguhr	8.61	1,633	0.825	7.9*	875	85.5	0.50†

*This cake was made from reused kieselguhr and was circulated for several hours through the mixing-pump system; changes in particles may have occurred.

†Estimated value from Brownell-Katz correlation, Equation (3); all other f values measured.

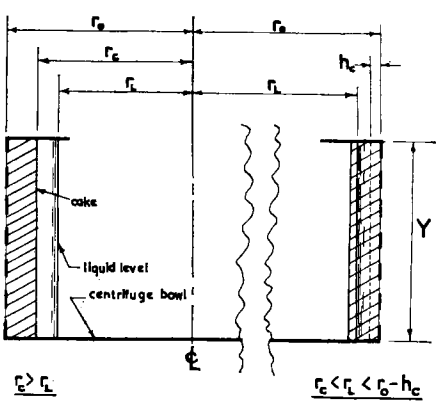

Fig. 18. Sketch of hydroextractor cake.

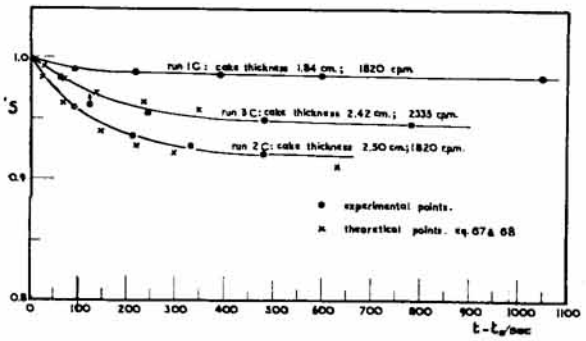

Fig. 19. Centrifugal drainage of water from chalk cakes in a 9-in.-diameter hydroextractor.

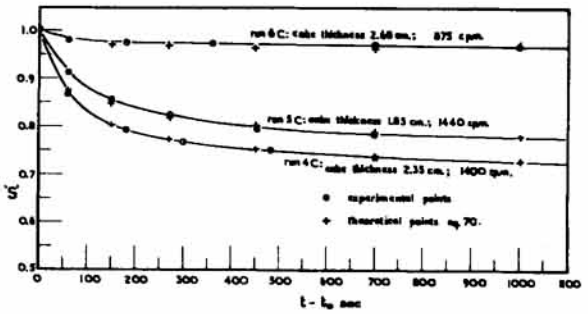

Fig. 20. Centrifugal drainage of water from kieselguhr cakes in a 9-in.-diameter hydroextractor.

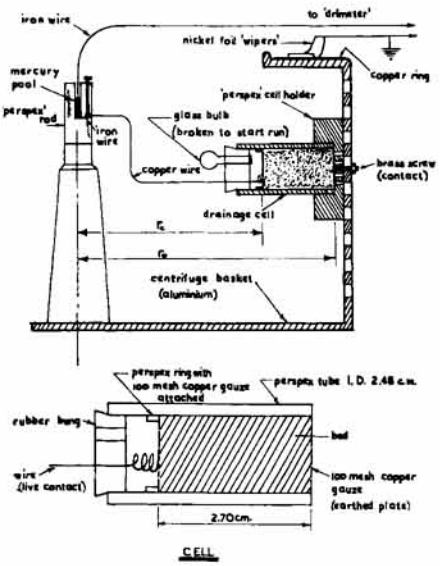

Fig. 21. Small capacitance cell held in hydroextractor for drainage of glycerol through glass ballotini.

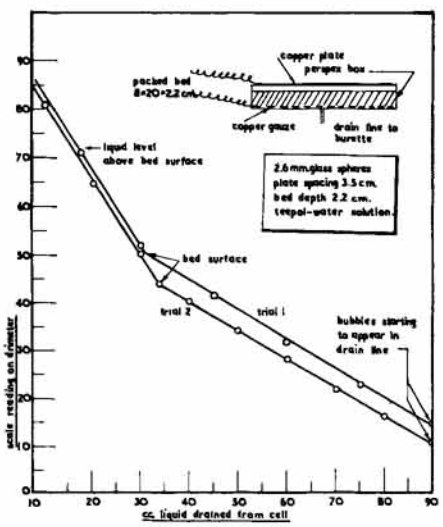

Fig. 23. Capacitance apparatus for gravity drainage from packed bed.

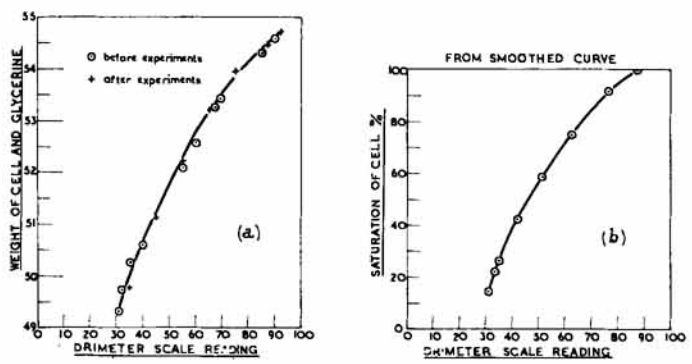

Fig. 22. Calibration of small-capacitance cell with glycerol.

to apply the capacitance method to complete cakes in the 9-in. hydroextractor. A fundamental problem appears to need solution. The electrical method proved successful in a small drainage cell (Figure 21) as it had done for drainage from beds of large particles in a gravitational field (Figure 23), giving clear indication of the point where the liquid level entered the surface of the bed and of the porosity relationship above and below the bed. The cell principle in Figure 21 was applied to the hydroextractor (Figure 24). The drainage curve from the Drimeter chart was as exemplified in Figure 25. The $S = 1$ position was indefinite and was found by extrapolation. The S, t curve for $S < 1$ was very shallow and fitted neither Equation (17), adjusted for G, to represent zero film drainage at the beginning of drainage just after $S = 1$, nor Equation (70) for purely film drainage toward the end of the drainage. It is clear that no fit could be obtained with the series solution which uses the limiting functions shown.

Although the chalk cake was spun for ten minutes at $N = 2{,}500$ rev./min. while submerged before the drainage test, shrinkage may be the problem when $S < 1$. Another possibility of error lies in the assumed proportionality between Drimeter scale reading and S over the range from $S = 1$ found by extrapolation in Figure 25a to fix t_0 and the measured value S_∞ after long spinning of the cake. This electrical method of following the S, t history of the cake requires further investigation as it does offer a possible method for following the chronological series of operations in a batch hydroextraction operation. If successful, it could then provide the major experimental method for the final functions proposed for the analysis and control of either batch or continuous operation.

Procedure and Results of Capacitance Cell

The procedure in a drainage run consisted of saturating the cell with an aqueous solution of glycerine and sealing the end with a small glass bulb. The cell was fixed in the centrifuge, and, when the basket had attained the desired constant speed, the bulb was broken. As the liquid level then moved toward the bed, the drainage started with $r_L < r_c$. Figures 26, 27, and 28 show data from runs at different speeds with glycerine-water solutions of various kinematic viscosities.

The curves drawn were calculated from values of capillary suction height h_c and permanent residual moisture f obtained from the Dombrowski-Brownell correlation, with a permeability K from the Kozeny equation. Actual measurements showed the estimated h_c as 2% high and the estimated K as 4% low. These discrepancies would have small effect on the S curve and show the value of the estimations. The estimated f values were not checked, as the long time required to attain S_∞ also allowed significant pick-up of atmospheric moisture by the glycerine. It is clear that in run 2G (Figure 27) f has been underestimated, but the series solution gives a reasonable prediction of the S, t function. It is also clear that the simpler equation (70) for film drainage alone gives a fair approximation.

CONCLUSIONS

The experimental results appear to confirm the value of the drainage equations proposed. Packed beds are expected

to fall into three general cases, depending on the properties of the system:

1. For fine particulate material, such as chalk, the beds have low permeability, and it is necessary to use the series solution to predict the moisture content variation with time.

2. For beds of intermediate permeability where there is no negative root for b_1 in Equation (50), such as the kieselguhr cakes, it is possible to use the simplified expression such as Equations (56) and (70) where film drainage is dominant.

3. For beds of fairly large crystals, the permeability will be high, and the capillary drain height may be an insignificant fraction of the cake thickness. In this event the expression $[4/27(p^3/(b-a)) - k_c^2]$ will approach an infinite value, and the root b_1 of Equation (50) will be indeterminate. Obviously the drainage of the full pores will be rapid; Equation (70) will reduce to Equation (71), and S_∞ will be small. The strings of beads may be taken as an extreme example, equivalent to

$$S = S_\infty + \frac{k_c}{(t - t_0)^{\frac{1}{2}}} \qquad (71)$$

The present studies of the drainage mechanisms have confirmed the need for consideration of the allied fields of capillary suction height, permanent residual moisture, and film drainage. The equations derived have been successful in application to the problems of drainage in a gravitational and in a centrifugal-force field, but the important correlations of capillary suction height and permanent residual moisture are still inadequate. The drainage equations warrant further study, particularly in their application to spin-drying, but much depends on finding a satisfactory method of measuring the moisture content of a moving hydroextractor cake.

The correlation of capillary drain height with capillary drain number proposed by Dombrowski and Brownell seems valuable, although wide deviations exist for nonspherical particles, emphasizing the need for further study of the effects of porosity and sphericity. These factors are not adequately represented by the inclusion of permeability in the capillary drain number, as their influences on flow characteristics are not necessarily the same as those on the capillary properties of the bed. Where applicable, the capillary drain height is best determined with a Haines apparatus and may then be assumed constant throughout a uniformly packed bed. When Haines's method cannot be used, an estimate of h_c can be found from the change of gradient on the S, t curve as the liquid surface enters the packing.

The correlation for permanent residual moisture requires further study, and benefit should result from a detailed solution to the problem of the maximum

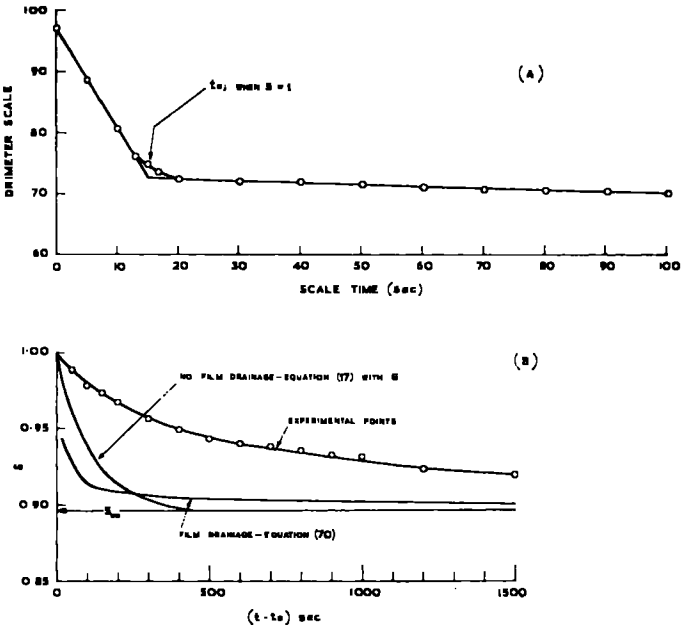

Fig. 25. Drainage test using capacitance measurement for water in chalk cake with N = 2,030, r_0 = 11.30 cm., r_c = 10.23 cm., ϵ = 0.615, K = 0.872 × 10^{-7} cc./sec.², S_∞ = 0.896 h_c = 0.87 cm., f = 0.20.

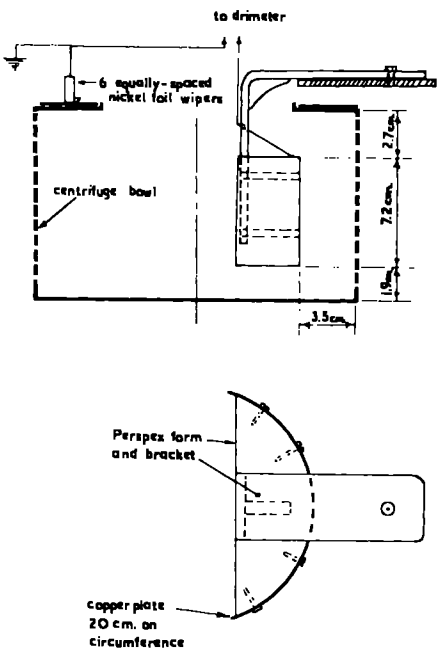

Fig. 24. Condenser arrangement in 9-in.-diameter hydroextractor, showing necessary earthing contact to copper ring pinned to the aluminum bowl.

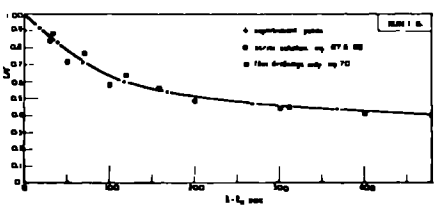

Fig. 26. Centrifugal drainage of glycerine solution from small cell, with N = 520 rev./min. and μ/ρ = 562 centistokes.

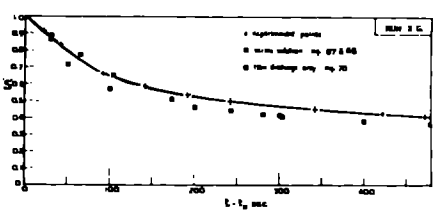

Fig. 27. Centrifugal drainage of glycerine solution from small cell, with N = 610 rev./min. and μ/ρ = 800 centistokes.

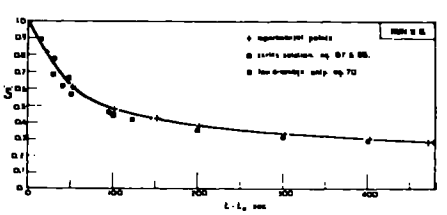

Fig. 28. Centrifugal drainage of glycerine solution from small cell, with N = 800 rev./min. and μ/ρ = 736 centistokes.

moisture retained at the contact point of two spheres. The velocity of drainage has only a minor effect on the retention.

Within these reservations on the accuracy of the values available for h_c and f, the series solution provides a saturation curve which applies to the drainage of beds for wide ranges of permeabilities and particle shapes. For beds of high permeability it is likely that the simple Equation (70) will apply. The relationships proposed have all depended on the assumption of a laminar flow regime, and this was found correct with the present materials. If with coarse particles in a centrifugal field, the flow in submerged pores becomes semiturbulent,

it is highly probable that drainage from the voids will be very fast and that Equation (70) will be valid for the major flow mechanism.

ACKNOWLEDGMENT

The research described above was carried out under an Imperial Chemical Industries Fellowship by one of the authors (E. Nenniger) in the Chemical Engineering Laboratory, Faculty of Technology, University of Manchester, England.

The authors are deeply indebted to Dr. L. R. Shenton, Senior Lecturer in Mathematics in the same Faculty, for his interest in this work. The successful solution obtained for the drainage equations was the result of tests of series solutions with various properties under his guidance.

NOTATION

A = area of packed bed normal to flow, sq. cm.
A_m = mean area of centrifuge cake, sq. cm.
a = constant for a given gravity-drainage run $a = h_c\rho KA/H\mu Q_s$ sec.$^{-1}$
a_c = constant for a given centrifuge run $a_c = h_c\rho KA/(r_0 - r_c)\mu Q_s$ sec.$^{-1}$
$a_1, a_2, a_3 \ldots$ etc. = series terms
B = film-drainage constant for a given run
b = constant for a given gravity drainage run $b = \rho KA/\mu Q_s$ sec.$^{-1}$
b_c = constant for a given centrifuge run $b_c = G\rho KA_m/\mu Q_s$ sec.$^{-1}$
$b_1, b_2, b_3 \ldots$ etc. = series terms
C_1 = constant in Batel's (*3*) correlation of capillary drain height
$c_1, c_2, c_3 \ldots$ etc. = series terms
d = particle diameter, cm.
d_m = mean particle diameter, cm.
d_h = diameter of maximum frequency in size distribution, cm.
f = permanent residual moisture as a fraction of voidage
G = acceleration force divided by g g./g.
g = acceleration of gravity—980 cm./sec.^{2}
H = depth of bed, cm.
h_c = capillary drain height, cm. fluid
h_L = height of liquid level above bottom of bed, cm.
K = bed permeability cc./sec.^{2}
k_1 = constant for a given gravity drainage run $= 2[s_0/3\epsilon]\sqrt{h\mu/\rho g}$
k_c = constant for a given centrifuge run $= 2[s_0/3\epsilon]\sqrt{(r_0 - r_c)\mu/G\rho g}$
k_4 = correction factor to Kozeny equation
k_5 = function of sphericity and voidage
L' = depth of bed in Dombrowski and Brownell (*8*) and Brownell and Katz (*4*) equations
L = equivalent horizontal width of draining film, cm.
N = revolutions per minute, min.$^{-1}$
n = revolutions per second, sec.$^{-1}$
ΔP = pressure drop across bed
p = constant for a given drainage, $p = (1 - f)$
Q = total volume of liquid above bottom of bed, cc.
Q_c = capillary-height volume $= h_c\, A\epsilon$, cc.
Q_s = total volume of voids in bed, cc.
Q_∞ = final volume of moisture content in drained bed, cc.
q = flow rate of liquid through the bed, cc./sec.
r_c = radius of inner face of centrifuge cake, cm.
r_L = radius of liquid level in centrifuge, cm.
r_0 = radius of outer face of centrifuge cake, cm.
S = total volume of liquid above base of bed divided by pore volume, i.e., $S > 1$ when $h_L > H$ and $S < 1$ when $h_L < H$
S_c = capillary height volume divided by total pore volume; $S_c = h_c/H$
S_r = total final residual moisture in Brownell and Katz (*4*) correlation $(= S_\infty)$
S_∞ = final volume of moisture content in drained bed divided by pore volume
s_0 = surface area per unit volume of bed, sq. cm./cc.
t = time, sec.
t_0 = time at which bed was saturated (i.e., $S = 1$), sec.
t_f = age of film, sec.
u = velocity of a point in the fluid in the x direction
v = velocity of a point in the fluid in the y direction
V_f = volume of liquid in the film, cc.
w = velocity of a point in the fluid in the z direction
X = variable in a gravity drainage run, $X = [1 - h_L/H]$
X_c = variable in a centrifuge run $X_c = [1 - (r_0 - r_L)/(r_0 - r_c)]$
X_∞ = final value of X, $X_\infty = 1 - S_c$
x = horizontal co-ordinate perpendicular to plane of wall where drainage is occurring
Y = vertical depth of centrifuge bowl, cm.
y = vertical coordinate measured downwards from top of film
z = horizontal coordinate parallel to wall where drainage is occurring
z_0 = capillary number

Greek Letters

α = contact angle
γ = surface tension, dynes/cm.
ϵ = void fraction
θ = function of b_1
μ = liquid viscosity, poise
ρ = liquid density, g./cc.
ρ_s = solid density, g./cc.
ϕ = film thickness, cm.
ψ_0 = solution to drainage equation neglecting film drainage in terms of t, sec.
ψ_1 = correction to t accounting for film drainage, sec.

LITERATURE CITED

1. Bashforth, Francis and Adams, J. C., "Capillary Action," Cambridge Univ. Press, (1883).
2. Batel, W.; *Chem. Ing. Tech.*, **26**, 497 (1954).
3. *Ibid.*, **27**, 497 (1955).
4. Brownell, L. E., and Katz, D. L., *Chem. Eng. Progr.*, **43**, 601 (1947).
5. Buckingham, Edgar, *U. S. Bur. Chem. and Soils Bull.*, **38** (1907).
6. Burak, Nathan, and Storrow, J. A., *J. Soc. Chem. Ind.*, **69**, 8 (1950).
7. Dallavalle, J. M., "Micromeritics," Pitman Pub. Co., New York, 220 (1943).
8. Dombrowski, H. S., and Brownell, L. E., *Ind. Eng. Chem.*, **46**, 1207 (1954).
9. Fisher, R. A., *J. Agr. Sci.*, **16**, 492 (1926).
10. Ferguson, Allan, *Phil. Mag.*, **26**, 925 (1913).
11. Gardner, Willard, and Widstoe, J. A., *Phys. Rev.*, **18**, 206 (1921).
12. Green, W. H., and Ampt, G. A., *J. Agr. Sci.*, **4**, 1 (1911).
13. Hackett, F. E., *Trans. Faraday Soc.*, **17**, 260 (1921).
14. Haines, W. B., *J. Agr. Sci.*, **17**, 264 (1927).
15. *Ibid.*, **20**, 96 (1930).
16. Haruni, M. M., and Storrow, J. A., *Ind. Eng. Chem.*, **44**, 2751 (1952).
17. *Ibid.*, 2756.
18. *Ibid.*, 2764
19. ———, *Chem. Eng. Sci.*, **1**, 154 (1952).
20. *Ibid.*, **2**, 108 (1953).
21. *Ibid.*, 164.
22. *Ibid.*, 204.
23. Haruni, M. M., and Storrow, J. A., *Chem. Eng. Sci.*, **3**, 43 (1954).
24. Haruni, M. M., J. A. Storrow, and K. H. Todhunter, *ibid.*, **3**, 87 (1954).
25. Hewitt, G. F. (Chem. Eng. Lab., Faculty of Technol. Univ. Manchester), Private communication (1956).
26. Jeffreys, Harold, *Proc. Cambridge Phil. Soc.*, **26**, 204 (1930).
27. Keen, B. A., *J. Agr. Sci.*, **14**, 177 (1924).
28. King, F. H., *U. S. Geol. Survey, 19 Ann., Rpt.*, II, 59 (1899).
29. Kocatas, B. M., and David Cornell, *Ind. Eng. Chem.*, **46**, 1219 (1954).
30. Morey, F. C., *Natl. Bur. Standards J. Research*, **25**, 385 (1940).
31. Nenniger, Emile, Ph.D. thesis, Univ. Manchester, (1956).
32. Nusselt, W., *Z. Ver. deut. Ing.*, **60**, 541 (1916).
33. Puri, A. N., "Soils—Their Physics and Chemistry," Reinhold Pub. Co., New York, 346 (1949).
34. Rose, H. E., *J. Appl. Chem.*, **2**, 511 (1952).
35. Storrow, J. A., *A.I.Ch.E. Journal*, **3**, 528 (1957).
36. Uren, L. C., and Difrawi, A. H., "Petroleum Development and Technology in 1926," Pet. Div. Am. Inst. Mining Met. Engrs.
37. Washburn, E. W., *Phys. Rev.*, **17**, (2nd Ser.), 273 (1921).

Manuscript received July 10, 1957; revised Nov. 27, 1957; accepted Nov. 29, 1957.